Papers from the

SEVENTH INTERNATIONAL SYMPOSIUM ON AIR BREATHING ENGINES

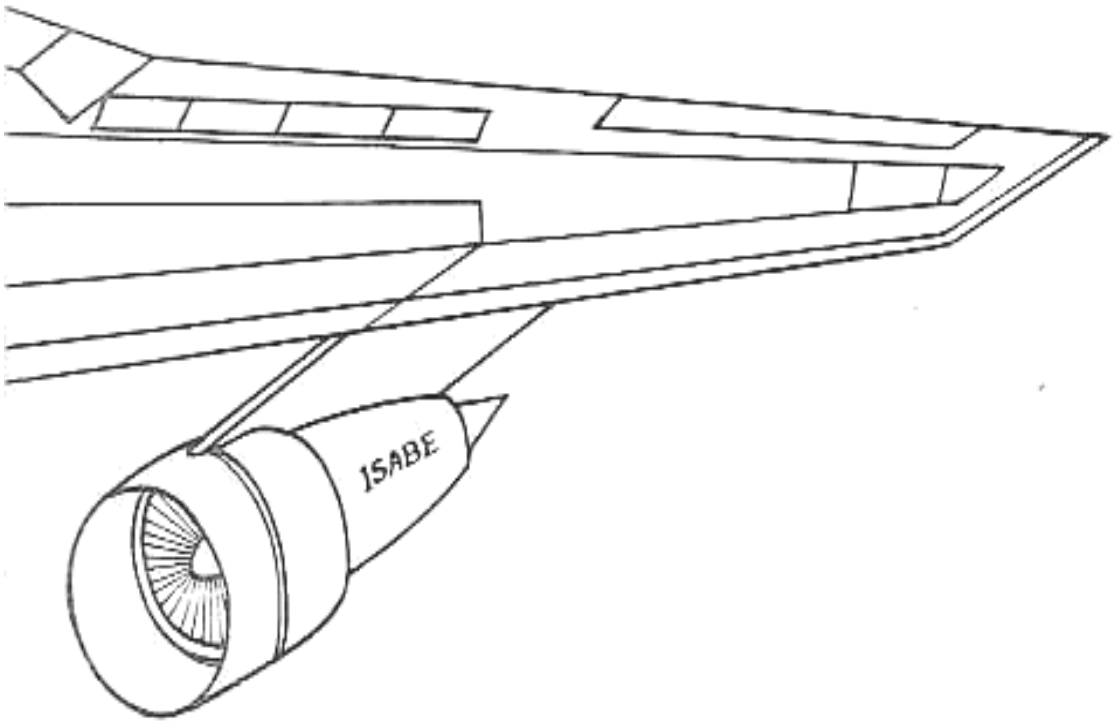

Organized by
THE CHINESE SOCIETY OF ENGINEERING THERMOPHYSICS

September 2-6, 1985
Beijing, People's Republic of China

Published and distributed by
American Institute of Aeronautics and Astronautics
1633 Broadway
New York, New York 10019

VON KARMAN INSTITUTE FOR FLUID DYNAMICS
TURBOMACHINERY LABORATORY
CHAUSSÉE DE WATERLOO, 72
B - 1640 RHODE SAINT GENÈSE - BELGIUM

PREPRINT 1985-15

EXPERIMENTAL CONVECTIVE HEAT TRANSFER INVESTIGATION AROUND A FILM COOLED HIGH PRESSURE TURBINE BLADE

C. CAMCI, T. ARTS, F.A.E. BREUGELMANS

PAPER PRESENTED AT THE 7TH INTERNATIONAL SYMPOSIUM
ON AIR BREATHING ENGINES
BEIJING, PEOPLE'S REPUBLIC OF CHINA
SEPTEMBER 2-6, 1985

TUT 8501/CC-TA-FAEB/LK

TABLE OF CONTENTS

EXPERIMENTAL CONVECTIVE HEAT TRANSFER INVESTIGATION AROUND A FILM COOLED HIGH PRESSURE TURBINE BLADE

C. CAMCI, T. ARTS, F.A.E. BREUGELMANS
VON KARMAN INSTITUTE FOR FLUID DYNAMICS
B-1640 RHODE SAINT GENÈSE - BELGIUM

Abstract

This paper deals with an experimental heat transfer investigation around a film cooled, high pressure gas turbine rotor blade. The measurements were performed in the von Karman Institute short duration isentropic light piston compression tube facility using platinum thin film gauges painted on a blade made of machinable glass ceramic. The coolant was ejected simultaneously through the leading edge (3 rows), the suction side (2 rows) and the pressure side (1 row). The coolant hydrodynamic behaviour is described and the effects of overall mass weight ratio, coolant to free stream temperature ratio and free stream turbulence are successively investigated.

List of Symbols

$\bar{c}$	blade chord
$\bar{c}_D$	mean value of the discharge coefficient
d	ejection hole diameter
$\bar{d}$	exit hole diameter of the shaped hole
h	convective heat transfer coefficient
i	incidence angle
LP,LM,LS	leading edge ejection rows
M	Mach number
m	blowing rate
$\dot{m}$	mass flow rate
P	pressure side ejection row
p	pressure
Re	Reynolds number
S	suction side ejection rows
s	curvilinear coordinate measured,from row LM, along the blade surface (+ along the suction side;- along the pressure side)
T	temperature
T_{ref}	reference temperature (= 290 K)
Tu	free stream turbulence intensity ($=\sqrt{\overline{u'^2}}/\bar{u}$)
u	velocity
u'	fluctuating component of velocity

Subscripts

c	coolant flow condition
∞	free stream flow condition
o	total condition
is	isentropic

1. INTRODUCTION

The most classical way to improve the thermal efficiency of a Joule/Brayton cycle is to increase the turbine entry temperature and pressure ratio. As a result, specific fuel consumption, size and weight of aero-engines have been significantly reduced during the last two decades. A 25/1 pressure ratio and a 1800 K turbine entry temperature are typical values observed in high performance jet engines [1]. However, these inlet free stream conditions are limited by material properties and an efficient blade cooling is most often required. Over the last years, a popular method to overcome the high temperature operation problems has been discrete hole film cooling.

In the severe engine environment of a film cooled airfoil, the large temperature differences existing between the mainstream and the blade surface induce a wall temperature pattern quite different from an adiabatic distribution. Considering the important spatial temperature variations due to internal cooling passages and the strongly varying heat flux distribution downstream of an ejection site, the most representative heat transfer quantity seems to be the convective heat transfer coefficient h, defined from the local wall heat flux, the mainstream recovery temperature and the local wall temperature, for given values of the blowing rate and the coolant temperature. As a matter of fact, either an experimental or a numerical determination of h is essential to perform any detailed heat conduction or thermal stress analysis.

Detailed short duration heat transfer measurements along the suction side of a film cooled rotor blade were performed by the present authors [2]. A numerical prediction of the wall heating rates, with and without film cooling, was attempted and use was made of a two dimensional boundary layer code [3] using an experimentally determined mixing length augmentation model. In spite of the simplicity of the numerical approach, computed and measured results compared quite well in a rather large range of blowing rates and temperature ratios. A detailed experimental heat transfer investigation around the leading edge of the same profile was also conducted by the present authors [4]. The effects of mass weight ratio, coolant temperature and incidence angle were successively investigated. Several other turbine blade film cooling studies are available in the literature [e.g., 5,6]. Quantities such as adiabatic wall temperature T_{aw} and adiabatic wall effectiveness η_{aw}, directly related to an adiabatic wall configuration, have most often been presented. Some typical examples in this research area are a detailed interpretation of curvature effects on the coolant film behaviour [7], the effect of curvature on η_{aw} [7,8], the rotational effects on film cooling [9], etc.

The aim of the present heat transfer investigation is to look at the multi-location, discrete hole film cooling of a high pressure rotor blade mounted in a 6-blade, stationary, linear cascade arrangement and submitted to correctly simulated flow conditions, i.e.,Mach and Reynolds numbers as well as free stream/wall/coolant temperature ratios. The mainstream flow is generated in the VKI isentropic light piston compression tube and the coolant is ejected simultaneously through the leading edge, the suction side and the pressure side. The hydrodynamic behaviour of the coolant plenum chambers and the heat transfer evolution without and with film cooling were successively investigated in a wide range of coolant to free stream mass weight and temperature ratios. The influence of free stream turbulence on film cooling heat transfer.

was also considered.

2. EXPERIMENTAL APPARATUS

2.1 Test facility

A short duration measurement technique was applied and use was made of the VKI isentropic compression tube facility. The operation principles of this kind of tunnel were developed by Schultz et al. [10] about 10 years ago. The VKI CT-2 facility [11] (Fig. 1), constructed in 1978, consists of a 5 m long, 1 m

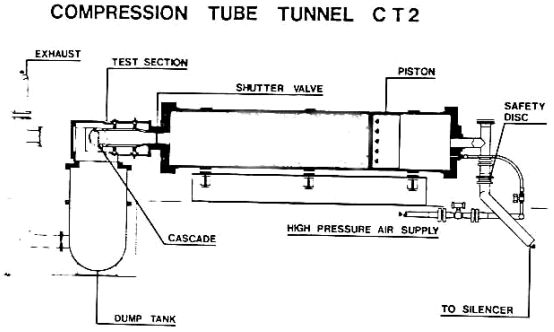

Fig. 1 - VKI isentropic compression tube facility

diameter cylinder containing a light weight piston, driven by the air of a high pressure reservoir. This cylinder is isolated from the test section by a fast opening slide valve. As the piston moves, the gas in front of it is nearly isentropically compressed until it reaches the pressure, and hence temperature, levels defined by the operator. The fast opening valve is then actuated by means of a detonator, allowing this pressurized air to flow through the test section. Constant free stream conditions are maintained in the test section until the piston completes its stroke. The maximum test section dimensions are 250×100 mm^2. The free stream gas conditions can be varied between 300 and 600 K and 0.5 and 7 bar. A 5 m^3 dump tank allows downstream pressure adjustments between 0.1 and 4 bar. A typical test duration is about 400... 500 ms. Further details about this facility and its operating principles are described in [10,11,12,13].

2.2 Data acquisition facility

All the pressure, temperature and heat flux measurements were directly acquired by a digital PDP 11/34 computer by means of a high speed data acquisition system. This unit, designed and built at VKI, is characterized by three separate sections. The first one consists of 24 analog circuits, which provide the transformation of the heat flux gauge signals, proportional to the wall temperature into signals proportional to the wall heat flux. The second section is composed of a series of 48 amplifiers and low-pass filters. The last section consists of three analog to digital converters, a multiplexer and a buffer. The signals are digitized using 12 bit words. This data acquisition facility can operate on 48 channels, with a maximum sampling frequency as high as 500 kHz. For the present measurements, the sampling rate was selected to be 1 kHz.

2.3 Model description

All measurements reported in this paper were carried out on the same rotor blade section as tested by Consigny & Richards [14]. The cascade geometry is fully described in this reference and the cooling configuration is summarized in figure 2. The blade instru-

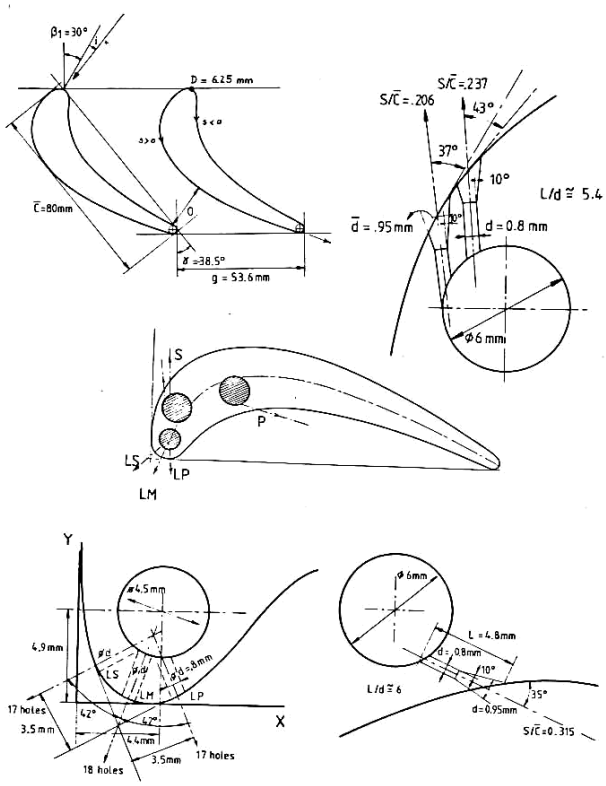

Fig. 2 - Cascade geometry and cooling configuration

mented for heat flux measurements was milled from "Macor" glass ceramic and 45 platinum thin films were painted on its surface (Fig. 3). Three rows of cooling holes (d=0.8 mm, $s/\bar{c}$=-0.031,0.,+0.031) are located around the leading edge (rows LP,LM,LS); the row and

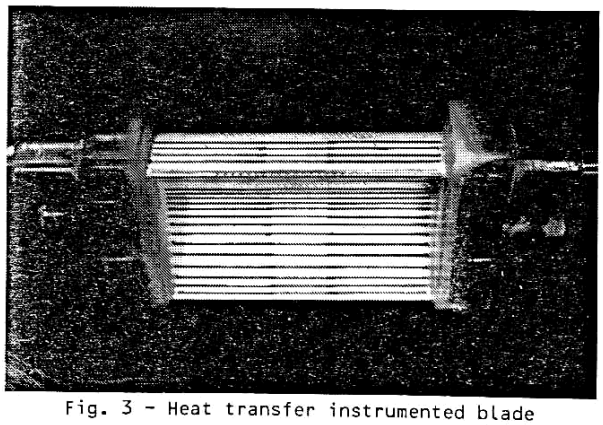

Fig. 3 - Heat transfer instrumented blade

hole spacing are both 2.48 mm. The holes are spanwise angled at 30° from the tangential direction. Two staggered rows of shaped holes (d=0.8 mm, $s/\bar{c}$=0.206,0.237) are located on the suction side (rows S); the row and hole spacing are respectively 2.48 mm and 2.64 mm. One row of shaped holes (d=0.8 mm, $s/\bar{c}$=0.315) is located on the pressure side (row P); the hole spacing is 2.64 mm. Three separate cavities are drilled along the blade height; they act as independent coolant plenum chambers. The coolant flow is supplied by a regenerative type cryogenic heat exchanger allowing a correct simulation of the coolant to free stream temperature ratio. Pressure tappings and miniature thermocouples provide continuously the coolant character-

istics at the 3 plenums inlet and outlet.

2.4 Measurement technique

The local wall heat flux is deduced from the corresponding time dependent surface temperature evolution, provided by the thin films. The wall temperature/wall heat flux conversion is obtained from an electrical analogy, simulating a one dimensional semi-infinite body configuration. A detailed description of this transient technique is given in references 15 and 13. The convective heat transfer coefficient is defined as the ratio of the measured wall heat flux and the difference between the free stream recovery and the local wall temperatures. A recovery factor equal to 0.896 is used, as if the boundary layer on the blade surface was turbulent everywhere. The uncertainties on the different quantities measured have been estimated as follows [4] :

h = 1000 W/m²K ±50W/m²K, except for the two gauges located in between rows LM,LP,LS
p = 2200 mm Hg ±15 mm Hg
T = 100 K ±0.5 K
$\dot{m}_c$ = 0.020 kg/s ±0.0005 kg/s
$\dot{m}_c/\dot{m}_\infty$ = 2% ±0.1%

2.5 Free stream turbulence generation

The free stream turbulence was generated by a grid of spanwise oriented bars. The turbulence intensity was varied by displacing the grid upstream of the model; a maximum of 5.2% was obtained. The natural turbulence of this facility is about 0.8%. The turbulence level, defined in the present paper as $\sqrt{u'^2}/u$, was measured using a VKI manufactured constant temperature hot wire probe.

3. DESCRIPTION OF THE MAINSTREAM FLOW

The isentropic Mach number distribution measured along the profile at zero incidence is shown in figure 4. The isentropic inlet and outlet Mach numbers are respectively equal to 0.251 and 0.925. The flow accelerates quite regularly along the suction side up to transonic conditions close to the trailing edge. Along the pressure side, a velocity peak is predicted at $s/\bar{c}$=-0.08. More downstream, a favourable pressure gradient accelerates the flow up to the trailing edge. Because of the relatively small leading edge radius and fast response instrumentation requirements, detailed static pressure measurements near the stagnation point could unfortunately not be carried out. A two dimensional inviscid time marching code [16] provides a quite valuable prediction of this velocity distribution (Fig. 4). However, because of the weakness of this approach to accurately model a very low velocity region, a singularity method [17] was applied around the leading edge in order to obtain a better estimation of the stagnation point position. At zero incidence, the latter was calculated to be at $s/\bar{c}$ = -0.019, in between rows LM and LP. This suggests that, when no coolant is ejected through the leading edge, rows LM and LS may be considered as roughness elements to be felt by the suction side boundary layer whereas, along the pressure surface, the boundary layer behaviour would only be affected by row LP.

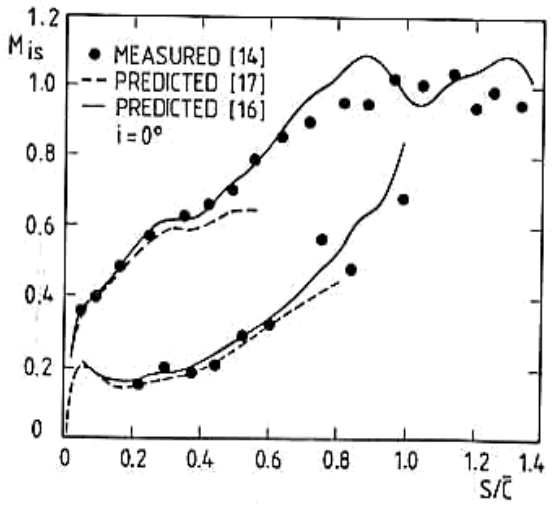

Fig. 4 - Blade velocity distribution

4. HEAT TRANSFER WITHOUT FILM COOLING

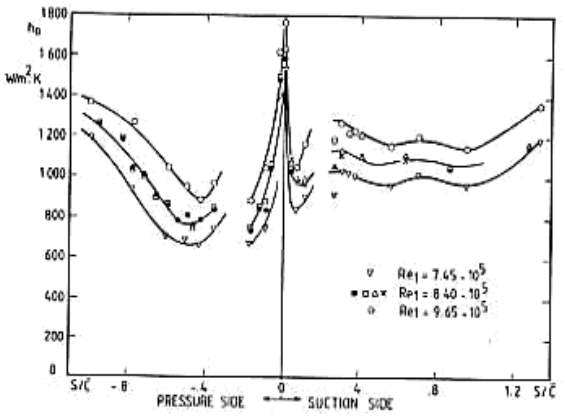

Fig.5-Heat transfer distribution without film cooling - Effect of Reynolds number

The convective heat transfer coefficient distributions measured at zero incidence, and without any coolant ejection, are shown in figure 5 for several free stream inlet Reynolds number values. A possible undesirable free stream air circulation was avoided by filling the three plenum chambers with flexible inserts. In the absence of the latter, as was demonstrated from oil flow visualizations [18],free stream air enters into the leading edge plenum through row LM; depending upon the local static pressures, it is ejected through rows LS and LP and strongly influences the local heat transfer rate.

The highest wall heating rates are measured in the leading edge region. The stagnation point heat transfer coefficient is proportional to the quantity $Tu_\infty Re^{1/2}$ as has been demonstrated by several experimenters [19,20]; a detailed investigation of the heat transfer around the leading edge of the present model, with and without cooling, is described in reference 4. Figure 6 demonstrates a definite influence of the existence of rows LM and LS on the transitional heat transfer distribution between $s/\bar{c}$=0.0 and 0.22 (suction surface ejection site). The comparison of the present data with those obtained by Consigny & Richards [14] around an identical but smooth, uncooled profile shows an earlier boundary layer transition, induced by the presence of the cooling rows LM and LS. A fully turbulent boundary layer is established at $s/\bar{c}$=0.25. Along the pressure side, the tripping effect of row LP is not as obvious. When the free stream turbulence intensity is equal to 5.2%, similar heat transfer distributions are measured around the present model and the one of Consigny & Richards. As a matter of fact, the early pressure side boundary

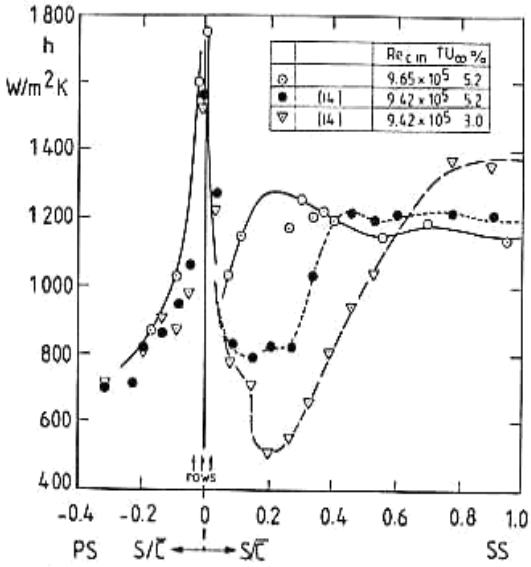

Fig.6-Heat transfer distribution without film cooling - Effect of cooling holes

layer transition is principally induced by the existence of a velocity peak and a curvature inversion; a breakdown of the three dimensional vortices originating from the stagnation region occurs, as mentioned in reference 21.

The boundary layers developing along the suction and pressure surfaces are much thinner than the ejection holes diameter. The boundary layer thickness computed at the location of the suction side ejection rows is about 5 times smaller than the hole diameter, corresponding to a local value of the hole diameter to momentum thickness ratio equal to 43, representative of a real situation. As a direct consequence, these boundary layers could undergo a local separation and reattachment over the suction and pressure side ejection rows; this behaviour explains the data scatter observed at the location of rows S and P (Fig. 5).

As already demonstrated by several investigators [22,23], a free stream turbulence variation only affects laminar or transitional boundary layers submitted to a favourable pressure gradient along curved surfaces. This behaviour is verified in figure 7. The effect of free stream Reynolds number is shown in figure 5. An increase of this quantity results in an overall enhancement of the heat flux level [2,21].

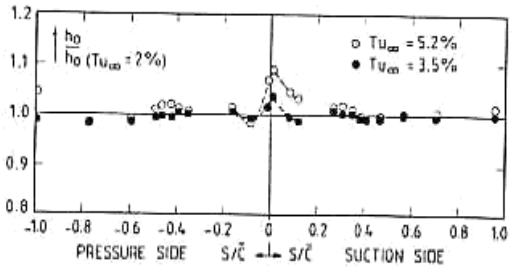

Fig.7-Heat transfer distribution without film cooling - Effect of turbulence intensity

5. COOLANT HYDRODYNAMICS

5.1 Total coolant mass flow rate

The coolant air ejected through rows P,LP,LM,LS and S is delivered by a single, common reservoir, through the heat exchanger providing the required coolant to free stream temperature ratio. The total coolant mass flow rate $\Sigma\dot{m}_c$, measured by means of a sonic orifice, is then shared between the suction side, leading edge and pressure side plenum chambers. The amount of coolant passing through each of these ejection sites must nevertheless imperatively be determined in order to evaluate the local coolant to free stream mass weight ratios and blowing rates. Since the total coolant mass flow rate is inversely proportional to $T_{oc}^{1/2}$, a normalized overall mass weight ratio $\left(\frac{\Sigma\dot{m}_c\sqrt{T_{oc}}}{\dot{m}_\infty\sqrt{T_{ref}}}\right)$ has been defined in order to establish a single functional dependency between the total coolant flow and the coolant to free stream pressure ratio (P_{oc}/P_∞). This dependency is shown in figure 8.

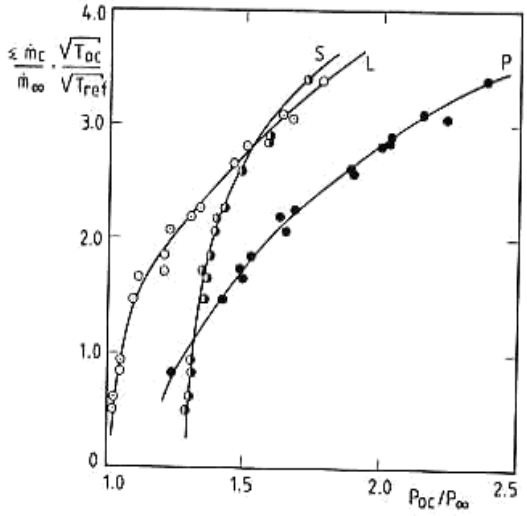

Fig. 8 - Normalized total coolant mass flow rate calculation

The results presented in the latter were obtained from the pressure and temperature measurements performed in each plenum, from the free stream static pressure evaluation at the location of each of the three ejection sites (Fig. 4) and from the measured total coolant mass flow rate. The measurements were taken for three different coolant to free stream temperature ratios ($T_{oc}/T_{o\infty}$=0.7,0.6,0.5).

5.2 Discharge coefficient

Mean values of the local discharge coefficient have been evaluated at the location of the pressure side, leading edge and suction side ejection rows from the independent film cooling investigations performed by the present authors [2,4,18]. The results of figure 9 were obtained. Significant losses are observed across the leading edge holes compared to the two other ejection sites. These values show, however, qualitative agreement with Tillman et al. data [24] obtained for a cylinder in cross flow configuration, but in a water tunnel rather than in a high speed compressible flow environment. The relatively low $\bar{C}_D$ values obtained in the leading edge region were expected to occur because of the highly complicated

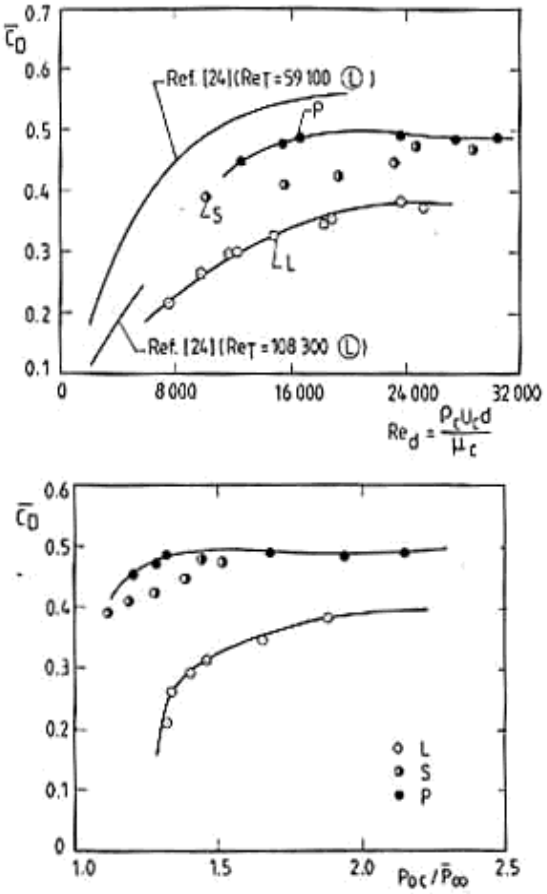

Fig. 9 - Discharge coefficients distribution

nature of the plenum chamber flow, with compound angle ejection through the three rows. Across the pressure and suction side rows, the C_D values vary between 0.4 and 0.5.

5.3 Coolant flow repartition

The quantitative determination of the coolant mass flow rate through each ejection site has been obtained by combining the data presented in figures 8 and 9. Using the information of figure 8, the value of the measured total mass flow rate, $\Sigma\dot{m}_c$, allows the evaluation of the coolant to free stream pressure ratio for each plenum and, hence, of the isentropic mass flux rate through the three ejection sites. Taking into account the corresponding discharge coefficients (Fig. 9) provides the three real mass flow rates. Each of these is characterized by the quantity $\frac{\dot{m}_{ci}}{\Sigma\dot{m}_c}$ (i=L,P,S) (Fig. 10). At very low pressure ratios, the flow conditions are not well defined in the leading edge plenum and very low C_D values are responsible for quite low local mass flow rates. The cooling rows S and P then perform the largest percentage of the ejection. However, for a typical value of the overall mass weight ratio $\left(\frac{\Sigma\dot{m}_c}{\dot{m}_\infty} = 0.03\right)$, the coolant split is found to be 40%/35%/25% respectively through the leading edge, suction and pressure side ejection rows.

5.4 Local blowing rates

The local blowing rates across the different ejection rows have been determined from the independent ejection mass flow rates (Fig. 10), the corresponding ejection area (Fig. 2) as well as from the local free stream conditions (Fig. 4). Because of very small free stream mass flux rates in the leading edge region and relatively small free stream mass flux rates along the first half of the pressure side, the rows LM and P eject the coolant at higher blowing rates (Fig. 11).

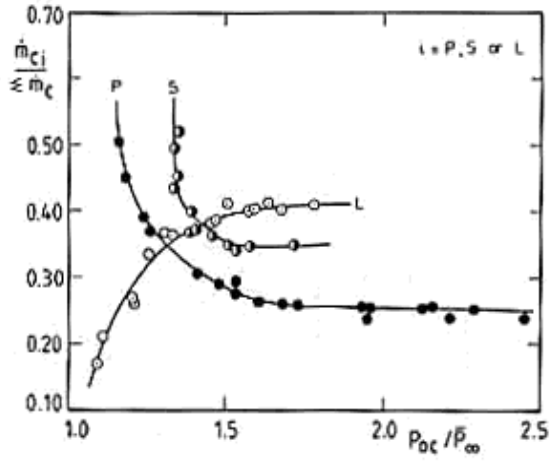

Fig. 10 - Coolant flow repartition

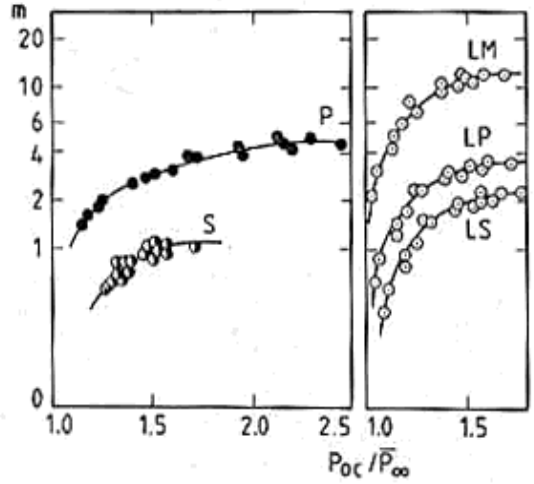

Fig. 11 - Local blowing rate evolution

6. HEAT TRANSFER WITH FILM COOLING

The heat transfer measurements with film cooling were performed at constant downstream Reynolds ($2.32\ 10^6$) and Mach (0.925) numbers. The free stream total temperature was equal to 415 K. The overall mass weight ratio was varied between 0.5% and 3.3% whereas coolant to free stream temperature ratios ranging between 0.51 and 0.70 were considered.

6.1 Heat transfer distribution downstream of row LS

The effect of overall mass weight ratio on the leading edge heat transfer distribution is shown in figures 12a,b,c. It should, however, be noted that

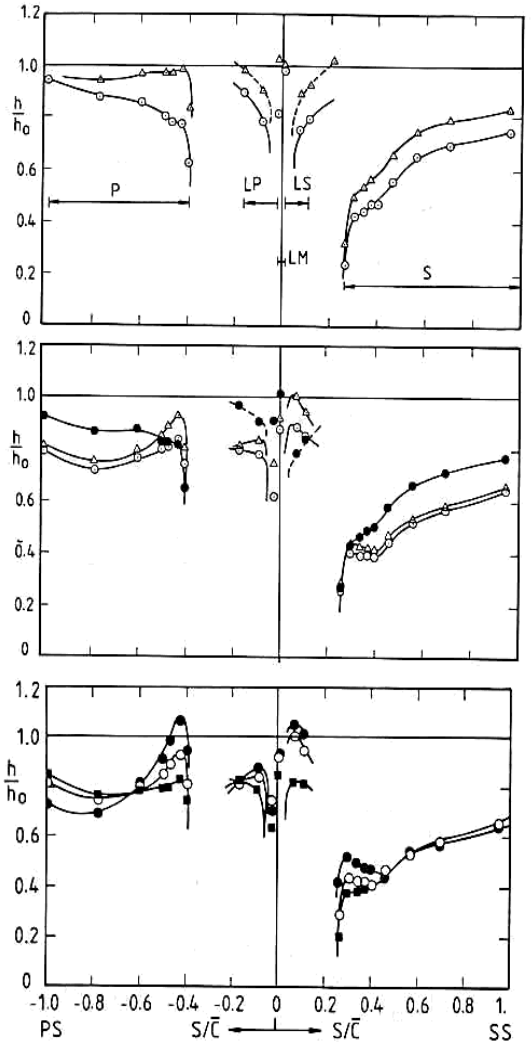

	$\dot{m}_c/\dot{m}_\infty$	$T_c/T_{0\infty}$	m_p	m_{LP} / P_{0c}/P_∞	m_{LM} / P_{0c}/P_∞	m_{LS} / P_{0c}/P_∞	m_s
△	0.50	0.71	1.42	/ 1.004	/ 0.984	/ 1.038	0.59
⊙	0.93	0.71	1.94	/ 1.022	/ 1.002	/ 1.056	0.62

	$\dot{m}_c/\dot{m}_\infty$	$T_c/T_{0\infty}$	m_p	m_{LP} / P_{0c}/P_∞	m_{LM} / P_{0c}/P_∞	m_{LS} / P_{0c}/P_∞	m_s
●	0.83	0.71	1.83	/ 1.017	/ 0.997	/ 1.052	0.62
⊙	1.66	0.70	2.70	0.88 / 1.070	3.02 / 1.050	0.56 / 1.107	0.71
△	2.07	0.70	3.03	1.74 / 1.209	5.98 / 1.186	1.11 / 1.251	0.72

	$\dot{m}_c/\dot{m}_\infty$	$T_c/T_{0\infty}$	m_p	m_{LP} / P^*	m_{LM} / P^*	m_{LS} / P^*	m_s
■	1.47	0.71	2.51	0.62 / 1.05	2.14 / 1.03	0.40 / 1.09	0.66
⊙	2.07	0.70	3.03	1.74 / 1.21	6.98 / 1.19	1.11 / 1.25	0.72
●	3.09	0.70	4.17	3.20 / 1.58	11.0 / 1.55	2.05 / 1.63	0.93

$P^* = P_{0c}/P_\infty$

Fig. 12 - Heat transfer distribution with film cooling - effect of overall mass weight ratio

the uncertainty associated with the measurements obtained from the two gauges located in between rows LM,LP and LS is quite high as they are affected by undesirable conduction phenomena as well as strong deviations from the assumed one dimensional heat transfer. For low overall mass weight ratio values (0.005...0.0093), the heat transfer behaviour is quite smooth downstream of row LS whereas, for higher values (1.47.. 3.09) a continuously increasing heat transfer augmentation is measured around $s/\overline{c}$=0.08. The latter is due to a high blowing rate ejection effect across a highly convex surface.

6.2 Heat transfer distribution downstream of row LP

Just downstream of row LP, the coolant layers developing around the leading edge are expected to lift off because of a strong convex curvature effect, especially at high blowing rates. This behaviour results in a local heat transfer augmentation measured at $s/\overline{c}\simeq$-0.8 (Fig. 12b,c) obviously function of the local blowing ratio. Downstream of the curvature inversion point, the effect of concave curvature is to induce the reattachment of the cold layers. The existence of a merging point, observed at $s/\overline{c}$=-0.16, and corresponding to tests with overall mass weight ratios equal to 0.0147, 0.0166, 0.0207 and 0.0309 confirms this assumption. A lower value of the overall mass weight ratio(< 0.010) provides a smooth heat transfer distribution (Fig. 12a).

6.3 Heat transfer distribution downstream of row S

The heat transfer distributions measured downstream of rows S at low overall mass weight ratios are shown in figure 12a. However, the suction side ejection rows blowing rate is nearly the same (0.59...0.62), a significant difference is observed in the heat transfer coefficient distribution. This might be explained by a cumulative effect, due to the action of the leading edge film, more effective for the highest value of the overall mass weight ratio. At higher overall mass weight ratios (Figs. 12b,c), a local wall heating augmentation, the strength of which being function of the local blowing rate value, occurs along the first 30 hole diameters downstream of rows S. This phenomenon is related to the very high local shear stresses and turbulent kinetic energy levels existing close to the wall. A second explanation might be the mainstream/wall interaction resulting from a severe jet penetration with a reduced lateral spread occurring along this convex surface. More downstream, no significant differences are observed : this is explained by the fact that the efficiency of the leading edge films is

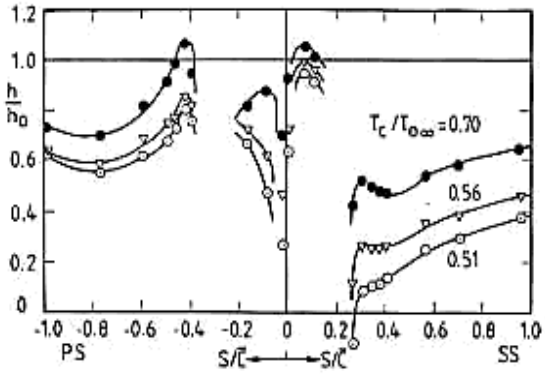

	$\frac{\dot{m}_c}{\dot{m}_\infty}$	$T_c/T_{0\infty}$	m_p	m_{LP} / p^*	m_{LM} / p^*	m_{LS} / p^*	m_s
●	3.09	0.70	4.17	3.20 / 1.58	11.0 / 1.55	2.05 / 1.63	0.93
▽	3.32	0.56	4.67	3.36 / 1.53	11.5 / 1.50	2.15 / 1.58	0.99
⊙	3.12	0.51	4.37	3.02 / 1.41	10.4 / 1.38	1.93 / 1.46	0.98

$p^* = P_{0c}/P_\infty$

Fig. 13 - Heat transfer distribution with film cooling - effect of temperature ratio

nearly independent from the local blowing rate and does not provide significant differences further downstream.

6.4 Heat transfer distribution downstream of row P

The total ejection area was chosen to supply the coolant flow at a high blowing rate, using forced reattachment to a concave surface considerations. At a very low overall mass weight ratio (≃ 0.005), an extremely low cooling effect is observed (Fig. 12a); the jets most probably move away from the blade surface. Increasing this value up to 0.0083...0.0147 improves the cooling efficiency, the jets are pulled down to the wall (Figs. 12a,b,c). However, if the overall mass weight ratio is raised to higher values, above 0.0166, the turbulence is locally augmented in a quite pronounced way just downstream of this ejection row, leading to appreciable heat transfer augmentations. Far downstream, however, the cooling is impresssively improved.

6.5 Influence of coolant temperature

Up to now, the tests were performed at a constant value of the coolant to mainstream temperature ratio ($T_{0C}/T_{0\infty}$=0.7) and only the effect of a varying overall mass weight ratio was considered. However, in a contemporary aero-engine, the coolant temperature is typically of the order of half of the mainstream one. In order to investigate the effect of this important parameter, measurements were performed for three different values of the coolant to free stream temperature ratio ($T_{0C}/T_{0\infty}$=0.7, 0.56, 0.51), whereas the overall mass weight ratio was kept constant. The heat transfer coefficient distributions of figure 13 were obtained.

Significant heat transfer reductions result from a lowering of the coolant temperature; only the suction side, downstream of LS, is less significantly affected, because of a too high local blowing rate, responsible for a jet separation. It is also interesting to note that downstream of rows P, LP and S, the wall heat flux augmentation, identified in a preceding section, decreases with the coolant temperature, although the local blowing rates are kept constant. This behaviour is due to the fact that a decrease of the temperature ratio results in an increase of the density ratio (ρ_c/ρ_∞) and hence, at constant blowing rate, in a decrease of the velocity ratio (u_c/u_∞) and moreover of the momentum flux ratio ($\rho_c u_c^2/\rho_\infty u_\infty^2$) and as a direct consequence, in a decrease of the turbulence augmentation downstream of an ejection row.

6.6 Influence of turbulence intensity

The effect of free stream turbulence intensity on the heat transfer with film cooling is shown in figure 14. The turbulence level was varied from 0.8% to 5.2% whereas the overall mass weight ratio and temperature ratio were kept constant. No significant changes in the wall heat flux are observed. This behaviour was expected because of the nature of the turbulent boundary layers developing around the blade profile.

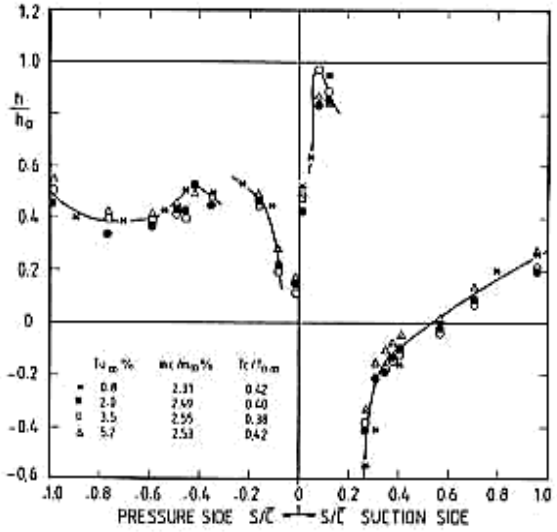

Fig.14 - Heat transfer distribution with film cooling - effect of turbulence intensity

7. CONCLUSIONS

Detailed heat transfer data have been obtained for a high pressure, film cooled rotor blade, looking at the influence of overall mass weight ratio, coolant to free stream temperature ratio and free stream turbulence intensity. The measurements were taken using the VKI short duration facility, under correctly simulated aero-engine conditions; the wall heat flux distributions were obtained from platinum thin film gauges painted onto a blade made of machinable glass ceramic. The coolant was ejected simultaneously through the leading edge (3 rows), the suction side (2 rows) and the pressure side (1 row).

The main conclusions of this investigation are :

a. Without coolant ejection

- Along the suction side, laminar to turbulent boundary layer transition is strongly influenced by the presence of the leading edge cooling holes, whereas

along the pressure side, the boundary layer behaviour is dominated by the free stream pressure gradient rather than by the existence of the cooling holes.

- The influence of free stream turbulence on the heat transfer coefficient distribution is quite limited. As expected, only the laminar and transitional regions, i.e., in the leading edge vicinity, are significantly affected.

b. With coolant ejection

- A normalized overall mass weight ratio has been defined, and making use of the local discharge coefficients, the local coolant mass flow and blowing rates have been obtained. A detailed evaluation of the 3 plenum chambers hydrodynamic behaviour has been presented.

- Film cooling around the leading edge has been proved to be quite effective at low overall mass weight ratios. At higher values, local heat transfer augmentations have been measured, as expected from an injection along a highly convex surface.

- Downstream of the pressure surface ejection row, pronounced wall heating augmentations have been identified; a very good wall protection was nevertheless obtained further downstream.

- Downstream of the suction surface ejection rows, the influence of overall mass weight ratio is limited within the first 30 hole diameters downstream of these rows. Higher blowing rates are again responsible for wall heat flux augmentation.

- A strong coolant temperature dependency on the overall heat transfer distribution has been observed whereas no significant effect of free stream turbulence was identified.

REFERENCES

1. OLSSON, U.: Advanced engine technology and its influence on aircraft performance. AIAA J.of Aircraft, Vol. 19, No 5, May 1982, pp 380-384.
2. CAMCI, C. & ARTS, T.: Short duration measurements and numerical simulation of heat transfer along the suction side of a film cooled gas turbine blade. ASME P 85 GT 111; also VKI Preprint 1984-33.
3. CRAWFORD, M.E.; KAYS, W.M.; MOFFAT, R.J.: Full coverage film cooling. Part II : Heat transfer data and numerical simulation. ASME Transact., Series A : J. Engrg for Power, Vol. 102, No 4, October 1980, pp 1006-1012.
4. CAMCI, C. & ARTS, T.: Experimental heat transfer investigation around the film cooled leading edge of a high pressure gas turbine rotor blade. ASME P 85 GT 114; also VKI Preprint 1984-32.
5. LANDER, R.D.; FISH, R.W.; SUO, M.: Experimental heat transfer distribution on film cooled turbine vanes. AIAA J.of Aircraft, Vol. 9, No 10, October 1972, pp 707-714.
6. MUSKA, J.F.; FISH, R.W.; SUO, M.: The additive nature of film cooling from rows of holes. ASME Transact., Series A : J.Engrg for Power, Vol. 98, No 4, October 1976, pp 457-463.
7. ITO, S.; GOLDSTEIN, R.; ECKERT, E.R.G.: Film cooling of a gas turbine blade. ASME Transact., Series A : J.Engrg for Power, Vol. 100, No 3, July 1978, pp 476-489.
8. RICHARDS, B.E.; VILLE, J.P.; APPELS, C.; SALEMI, C.: Film cooling of heated turbine surfaces at simulated conditions. AIAA P 77-947.
9. DRING, R.P.; BLAIR, M.F.; JOSLYN, H.D.: An experimental investigation of film cooling on a turbine rotor blade. ASME Transact., Series A : J.Engrg for Power, Vol. 102, No 1, January 1980, pp 81-87.
10. JONES, T.V.; SCHULTZ, D.L.; HENDLEY, A.D.: On the flow in an isentropic free piston tunnel. ARC R&M 3731, January 1973.
11. RICHARDS, B.E.: Heat transfer measurements related to hot turbine components in the von Karman Institute Hot Cascade Tunnel. in "Testing and Measurement Techniques in Heat Transfer and Combustion", AGARD CP 281, Paper 6, 1980; also VKI Preprint 1980-15.
12. SCHULTZ, D.L.; JONES, T.V.; OLDFIELD, M.L.G.; DANIELS, L.C.: A new transient facility for the measurement of heat transfer rates. in "High Temperature Problems in Gas Turbine Engines", AGARD CP 229, Paper 31, 1977.
13. LIGRANI, P.M.; CAMCI, C.; GRADY, M.S.: Thin film heat transfer gauge construction and measurement details. VKI Technical Memorandum 33, November 1982.
14. CONSIGNY, H. & RICHARDS, B.E.: Short duration measurements of heat transfer rate to a gas turbine blade. ASME Transact., Series A : J.Engrg for Power, Vol. 104, No 3, July 1982, pp 542-551.
15. SCHULTZ, D.L. & JONES, T.V.: Heat transfer measurements in short duration hypersonic facilities. AGARDograph 165, 1973.
16. ARTS, T.: Cascade flow calculations using a finite volume method. in "Numerical Methods for Flow in Turbomachinery", VKI LS 1982-05, April 1982.
17. VAN DEN BRAEMBUSSCHE, R.: Calculation of compressible subsonic flow in cascades with varying blade height. ASME Transact., Series A : J.Engrg for Power, Vol. 95, No 4, October 1973, pp 345-351.
18. CAMCI, C.: An experimental and theoretical heat transfer investigation of film cooling on a high pressure gas turbine blade. Ph.D. Thesis, Katholieke Universiteit Leuven, 1985 (to be published).
19. SADEH, W.Z.; BRAUER, H.J.; GARRISON, J.A.: Visualization study of vorticity amplification in stagnation flow. Colorado State U., SQUID-CSU-1-PU, Oct.1977.
20. KESTIN, J. & WOOD, R.T.: The influence of turbulence on mass transfer from cylinders. ASME Transact., Series C : J.Heat Transfer, Vol. 93, No 4, November 1971, pp 321-327.
21. DANIELS, L.C.: Film cooling of gas turbine blades. Ph.D. Thesis, Oxford U., Engrg Lab., Report No 1302/79, 1979.
22. BÜYÜKTÜR, A.R.; KESTIN, J.; MAEDER, P.F.: Influence of combined pressure gradient and turbulence on the transfer of heat from a plate. Int J. Heat & Mass Transfer, Vol. 7, No 11, November 1964, pp 1175-1186.
23. JUNKHAN, G.H. & SEROVY, G.K.: Effects of free stream turbulence and pressure gradient on flat plate boundary layer velocity profiles and heat transfer. ASME Transact., Series C : J. Heat Transfer, Vol. 69, No 2, May 1967, pp 169-176.
24. TILLMAN, E.S.; HARTEL, E.L.; JEN, H.F.: The prediction of flow through leading edge holes in a film cooled airfoil with and without inserts. ASME Paper 84 GT 4.